Experimental demonstration of a transient grating controlled all-optical switch

Engineering Research Express

PAPER

Experimental demonstration of a transient grating controlled all-optical switch

RECEIVED
14 October 2022

REVISED
2 February 2023

ACCEPTED FOR PUBLICATION
8 February 2023

PUBLISHED
16 February 2023

Osman Akin[1,*] **and Mehmet S Dinleyici**[2]

[1] Department of Mechatronics Engineering, Izmir Katip Celebi University, Cigli Campus, 35620, Izmir, Turkey
[2] Electrical and Electronics Engineering, Izmir Institute of Technology, Gulbahce Koyu, Urla, 35430, Izmir, Turkey
[*] Author to whom any correspondence should be addressed.

E-mail: osman.akin@ikcu.edu.tr

Keywords: fiber optic components, optical switching, nonlinear optics, kerr effect

Abstract

We demonstrate an on-fiber all-optical switching device based on a transient grating formed by the interference of control laser pulses in a Kerr-type nonlinear material placed in the evanescent region of the fiber. The device can operate in two distinctive modes. First, switching/coupling among the fiber modes using bulk index modulation was investigated and an efficiency of about %0.55 @852 nm was measured. Second, by exploiting Four Wave Mixing (FWM), an all-optical switching that transfers power among light signals with wavelengths of $\lambda_1 = 440$ nm and $\lambda_2 = 663$ nm was achieved by quasi-phase-matching and fRequency matching in a nonlinear thin polymeric film. The results prove that the introduced switching structure may have the potential to be used in integrated photonic applications such as intensity modulators or controllable couplers.

1. Introduction

The huge demand for higher bandwidth in current communication networks implies replacing conventional switching components with their all-optical counterparts operating at much higher speeds with lower power consumption. Considering an all-optical switching device, the signal-light propagation can be modulated via a control light by utilizing various third-order optical nonlinear effects. Traditional in-fiber devices are composed of a structure on the light path that induces phase shift, wavelength selection, or blocking function on the propagating wave. Numerous publications for all-optical switching are based on stationary gratings externally written on the fiber core [1]. The fundamental switching methodologies are coupler devices [2], semiconductor optical amplifiers [3], quantum dots [4], Mach–Zehnder Interferometers [5], and micromechanical optical switches where the optical grating is suspended on a moving platform above a waveguide [6]. The transverse mode conversion based on optically induced dynamic long-period gratings in fiber core has been demonstrated [7, 8]. All-optical switching devices can also be constructed using photonic (or plasmonic) micro/nano-structures as a matrix, containing nonlinear optical materials [9]. However, in some publications, it was proposed that a periodic static perturbation created in the cladding can affect the fundamental core mode strongly [10] and have the switching functionality with an extinction ratio of 28.8 dB [11, 12]. Controlling the power of propagating modes in fiber using conventional static gratings is a known process. However, the formation of a dynamic grating in the cladding using external control light may yield manipulating the power of propagating modes in the fiber or provide wavelength conversion in the fiber. The fiber mode is resonated in the transverse direction and that very sensitive state can easily be broken/cracked by changing the boundary condition at the cladding using a transient grating. The temporal nature of the applied pump signal can lead to designing of ultrafast signal processing structures for all-optical photonic devices.

Besides many physical phenomena used in optical device implementations, the Kerr effect is known as one of the fastest phenomena that can be exploited to design a high-speed all-optical switching mechanism [13, 14]. Transient grating formation using the Kerr effect in the bulk crystal was investigated by Schneider *et al* [15]. The utilization of polymeric materials in third-order nonlinear optical processes (Kerr type) offers great advantages

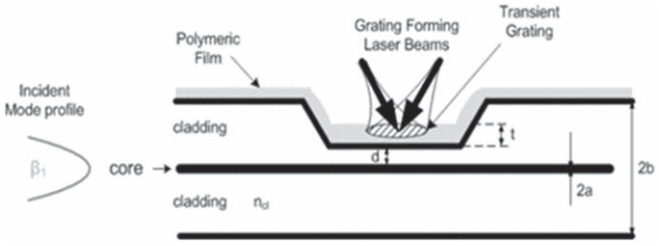

Figure 1. Illustration of the fiber switching device. (*Core refractive index:* 1.464@651nm, $NA = 0.14$, $2a = 5.3\mu$m, $2b = 125\mu$m, $d = 9.22\mu$m).

in terms of response time, high nonlinearity, and processing simplicity [16]. Organic polymeric materials exhibit strong optical nonlinearities and may be good candidates for all-optical switching devices. Some feasible techniques combining physical optical structures with nonlinear polymeric materials are proposed to achieve an all-optical integration as hybrid photonic components [17].

In this study, we demonstrate an ultrafast optical switch based on a coupler structure that comprises a nonlinear polymer slab waveguide layered on the side polished single-mode fiber as shown in figure 1.

The refractive index of the dye-doped polymer slab waveguide can locally be altered with a transient grating generated by the interference of control laser pump pulses. Refractive index modulation arising from the intensity-dependent Kerr effect becomes in the shape of the interference pattern profile of the control beams. The nonlinear medium enables the interaction of the propagating mode with the grating forming laser control light in the evanescent region of the waveguide that results in all-optical switching because of Four Wave Mixing (FWM) interactions. Because of the fast response time of Kerr-type materials, this method may provide the possibility to achieve high optical switching rates of about hundreds of Gbits/s. The mathematical model considering Four Wave Mixing (FWM) at the core-cladding boundary was shown in [18] where the power coupled into the higher-order propagating modes is computed using Coupled Mode Theory (CMT). Evanescent coupling at the interface of polymer slab waveguide and side-polished single-mode fiber was demonstrated in [19]. In this study, we employ the hybrid nonlinear polymer-silicon structure to realize experimentally an all-optical ultrafast switch based on a coupler structure.

2. All-optical switching based on a transient grating

The switching structure is formed by polishing the single-mode fiber cladding and replacing the polished part with a thin polymeric film. The length of the fiber (Corning HI1060) is 2 m, the polished cladding part is created just in the middle of the fiber, and the flattened region's length is about 10 mm. The distance between the core and the flat side of the fiber is 9.22 μm. The preparation of the nonlinear film used to form the slab waveguide layer is described in detail by He *et al* [20]. The thin film has a linear refractive index $n = 1.48$ which was estimated experimentally using the Fresnel diffraction-based nondestructive measurement method [21]. The Kerr coefficient of the polymeric film was measured using the Z-scan experimental technique and found to be $n_2 = -4.616 \times 10^{-11}$ cm^2 W^{-1}. To increase the nonlinearity and match the linear refractive index of the film, 20 nm SiO_2 particles with refractive indices of 1.46 @532 nm, [Alfa Aesar-Pr.No.12727] were added to the mixture of PVA and dye solutions such that nanoparticles and PVA weight equally (SiO2 - %7.35, PVA- %7.42, Methyl Red - % 0.014). The acquired mixture is coated onto the polished part of the fiber by the Doctor Blade method and dried for approximately 24h at room temperature. The resulting film has an approximate thickness of 17.83 μm.

Before utilizing in the fiber device, the transient grating formation on the film was tested using the conventional pump-probe technique and the efficiency of approximately 10% was measured.

2.1. Optical switching by mode conversion

Nonperiodic interference fringes inducing instantaneous switching are formed by crossing the two pump beams with a Gaussian profile on the polymeric film. These fringes take the form of transient refractive index modulation (perturbation) on the film due to the Kerr effect. Meanwhile, fiber modes propagating in the core interact with the transient grating, and Four-Wave Mixing occurs if the frequency and phase-matching requirements are satisfied.

In the experiment, depending on the grating structure parameters (grating period), the switching capability of the device is investigated. The experimental setup is depicted in figure 2. Three laser sources with wavelengths of 632.8 nm, 543 nm, and 852 nm are used separately to excite the fiber. The experiment aims to investigate the

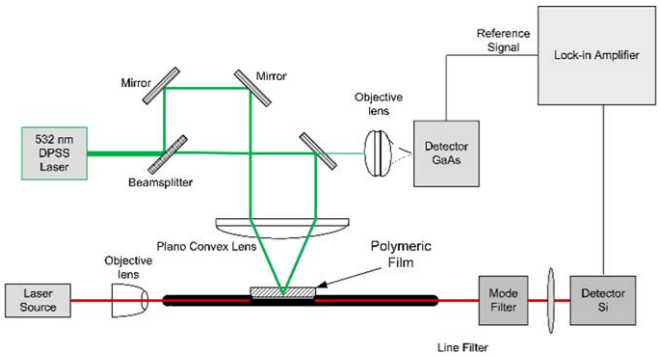

Figure 2. Switching with a transient grating.

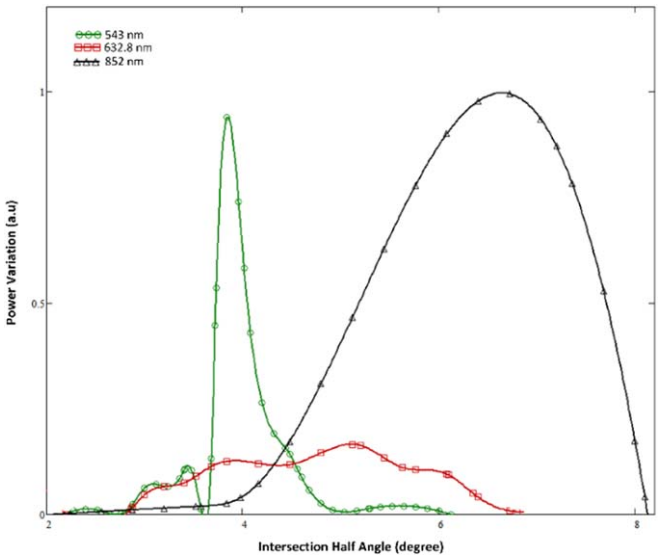

Figure 3. Output power variation as a function of interference angle at 543 nm (), 632.8 nm (), 852 nm ().

effect of the transient grating on the modes propagating in the waveguide. In all cases, the nearly single-mode excitation is ensured by observing the far-field radiation pattern on CCD [21]. To show the switching capability of the transient grating, an experimental setup given in figure 2 is constructed. A DPSS laser with 532 nm wavelength, a pulse width of 14 ns, a repetition rate of about 25 kHz, and a beam peak power of 1.994 kW is employed as a pump (control) beam source. The light output of the laser is split by a 50% beam splitter into two excitation beams and those beams are crossed on the polymer to form a transient grating. A Plano-Convex lens with a 5 cm diameter and 7.5 cm focal length is used to focus the pump beams. The pump beams are sent parallel to each other and the separation distance between the parallel beams is used to modify the interference angle. Each beam has a spot size of 1mm. The effect of transient grating on the propagating mode is measured using a high-speed Silicon PIN detector connected to Lock-In Amplifier. To begin with, the fiber modes are excited by the He-Ne laser with a 543 nm wavelength. The light that emerged from this laser is coupled to the fiber with an objective lens having an NA value of 0.11. By utilizing the Sellmeier approach, the fiber's core and cladding refractive indices at that wavelength are estimated as $n_{core} = 1.46372$ and $n_{cl} = 1.46151$, respectively.

According to these refractive index values, fiber supports two modes: LP_{01} mode with an effective index of 1.4627176 and LP_{11} modes with an effective index of 1.4615364. Here, the power at the output of the fiber is measured as 100 nW by the optical power meter. When the pump pulses are applied to the film, the transient grating is formed and the influence of the grating on the propagation mode is observed as a power variation at the fiber output as a function of the half intersection angle (grating period) that is given in figure 3. For half intersection angle of $\theta = 3.731°$, power variation of 0.336 nW is observed at the fiber output.

Subsequently, a He-Ne laser with 632.8 nm wavelength and 15 mW output power is employed as a light source. The fiber's core and cladding refractive indices at that wavelength are estimated as $n_{core} = 1.46277$, and

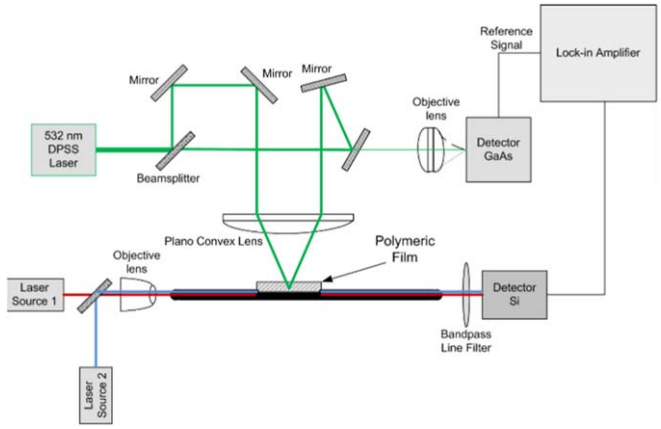

Figure 4. Wavelength switching with a transient grating.

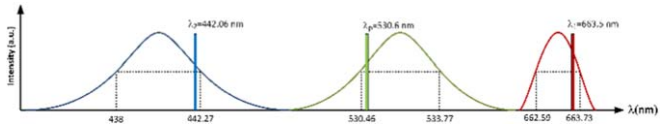

Figure 5. Laser sources bandwidths: green line - 532 nm DPSS laser; Red Line: 'Laser source 1'- Red laser diode; Blue line: 'Laser source 2'—Single-mode blue laser diode.

$n_{cl} = 1.45757$, respectively. Here, fiber supports two modes: LP_{01} mode with an effective index of 1.4611506 and LP_{11} mode with an effective index of 1.4588856.

The profile of launched beam at the far field is recorded by CCD and the power at the output of the fiber is measured as 342 nW. For half intersection angle θ of about 5.2° corresponding to 1.957 μm grating period, power modulation due to transient grating is measured at the fiber output. To proceed, another source with an 852 nm wavelength laser is utilized to launch the light into the fiber. The power meter reads 75 nW at the fiber output. The fiber's core and cladding refractive indices at that wavelength are estimated as $n_{core} = 1.4588$ and $n_{cl} = 1.45248$, respectively. In this case, fiber supports two modes: LP_{01} mode with an effective index of 1.4561920 and LP_{11} mode with an effective index of 1.4528941. For half intersection angle of about 5.2°, maximum power variation of 0.418 nW, which refers to %0.55 efficiency, is measured at the fiber output as shown in figure 3.

2.2. All-optical switching by wavelength conversion

The purpose of the setup given in figure 4 is to investigate the power transfer between different wavelengths due to Four Wave Mixing process occurring on the nonlinear polymer placed in the cladding. The light waves with wavelengths of $\lambda_1 = 633$ nm and $\lambda_2 = 440$ nm were launched into the fiber simultaneously and control pump beams with a wavelength of 532 nm were applied to the nonlinear material at the same time. According to the FWM theory, power exchange between propagating modes is expected in a nonlinear medium.

The power variation at every wavelength was measured using a lock-in amplifier as shown in figure 4.

A line filter with narrow bandwidth was utilized before the detector to block irrelevant wavelengths. The spectrum of the laser sources was characterized by Optical Spectrum Analyzer, and depicted in figure 5. The vertical lines given in the figure represent the wavelengths that can take a role in the interaction process, which are also described by the equation (3). The light beams from Source 1 (663 nm) and Source 2 (440 nm) were combined with a beam splitter and launched into the fiber using an objective lens with NA = 0.11, as given in figure 4. Nearly single-mode excitation for each of the laser sources was assured before the execution of the full experiment.

To begin with, the effect of grating on each wavelength was observed using a detector and lock-in amplifier at the fiber output. When only '*Laser source 1*' was launched, at half intersection angle of 7.1°, maximum power modulation of 40 pW was observed at the fiber output as shown in figure 6. This angle corresponds to the grating period of $\Lambda = 1.435$ μm and 1 mm grating length. In the second step, '*Laser Source 1*' was turned off and '*Laser Source 2*' with wavelength λ_2 was launched into fiber and the single mode was excited. In this case, a maximum

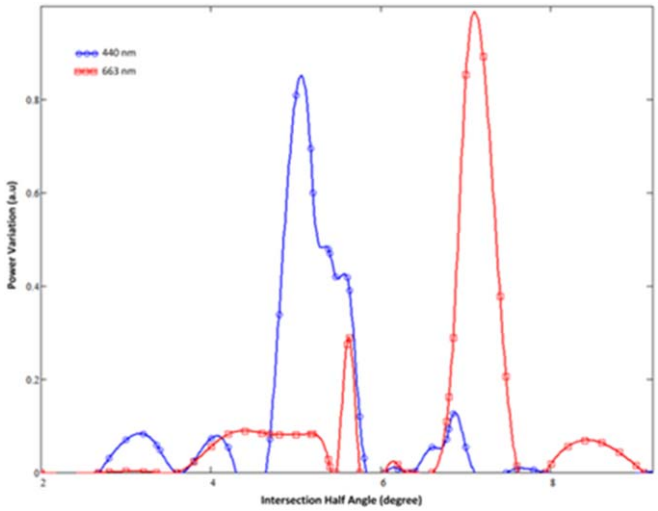

Figure 6. Output power variation as a function of interference angle at 663 nm (▭▭▭) and 440 nm (⊖⊖⊖).

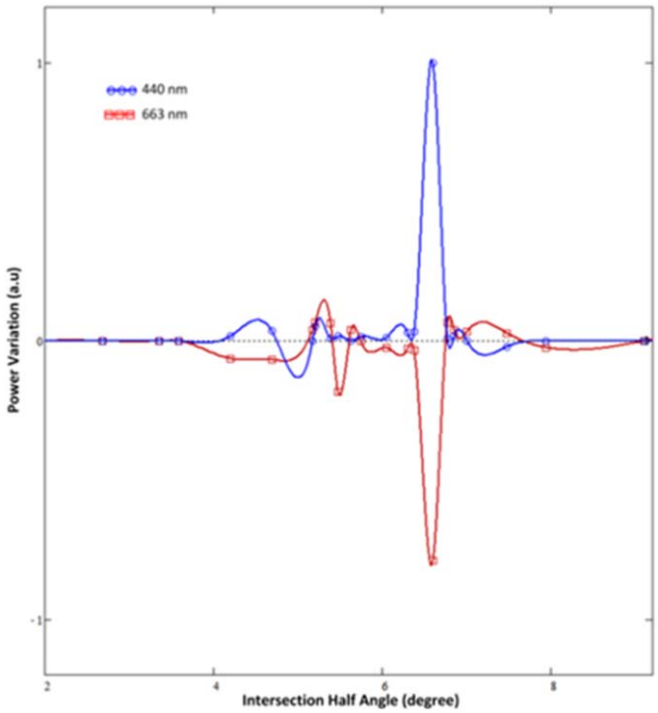

Figure 7. Wavelength conversion: power modulation at 440 nm (⊖⊖⊖) and 663 nm (▭▭▭).

power increase of 35 pW was observed at 5.06°. This angle corresponds to the grating period 2.01 μm and the grating length is about 1 mm. The power modulation according to the interference angle (grating period) is given in figure 6.

As a final step, two laser sources with distinct wavelengths of 663 nm and 440 nm were launched at the same time. Figure 7 indicates the power modulation at each wavelength at the output of the fiber, measured as a function of interference angle (grating period). The coupling in the structure begins in the vicinity of $\theta \approx 6.5°$ and at a half interference angle of 6.6°, the phase, and frequency matching conditions for Four Wave Mixing are satisfied and power transfer of $0.25nW$ from a signal with wavelength λ_1 into the signal with λ_2 was observed. The power transfer occurred from the stronger signal to the weaker one.

The grating period was 1.548μm and the grating length was measured as 1 mm.

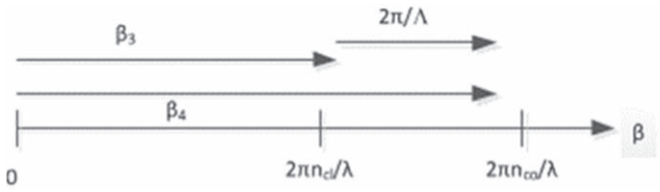

Figure 8. Demonstration of coupling using propagation constants.

Table 1. Classification of FWM interaction processes

	Frequency matching condition	Quasi-phase matching condition	Switching type
I	$\omega_4 = \lvert\omega_3\rvert$	$k_4 = k_3 \pm 2k_0 \sin\theta$ $k_4 = -k_3 \pm 2k_0 \sin\theta$	Mode Conversion Switching
II	$\omega_4 = \lvert 2\omega_0 - \omega_3\rvert$	$k_4 = \pm k_3$	Wavelength Conversion Switching
III	$\omega_4 = \lvert 2\omega_0 + \omega_3\rvert$	$k_4 = \pm k_3$	Wavelength Conversion Switching

3. Discussion

3.1. Discussion on optical switching by mode conversion

In the presence of a grating, the coupling of the mode with propagation constant β_m into the mode with propagation constant β_n occurs if the phase matching is satisfied [23]

$$\beta_n \pm \beta_m = \pm p\frac{2\pi}{\Lambda} \tag{1}$$

Where Λ as the grating period and p are positive integer numbers. The propagation constant can be written in terms of the effective index n_{eff} as

$$\beta = \frac{2\pi}{\lambda} n_{eff} \tag{2}$$

To understand the coupling mechanism, the phase matching conditions in aperiodic transient gratings were derived in [14].

Because of the lack of an exact analytical solution for the aperiodic structures, the grating function was extended into the Fourier series and coupling efficiencies for all the Fourier components were derived. When complete phase matching conditions are satisfied, a strong coupling is expected between the fiber modes. However, phase-matching requirements may also be satisfied only for some Fourier components, which results in weak coupling. This weak coupling mechanism is related to the shape (Gaussian-apodized, raised-cosine-apodized, etc) and the length of the transient grating as well as the grating period.

We used three different laser sources with wavelengths of 632.8 nm, 543 nm and 852 nm to investigate the optical switching mechanism using mode conversion. The grating has been generated by the 532 nm laser source as shown in figure 2.

Considering the switching structure shown in figure 2, for the source with $\lambda = 543$ nm, fiber supports two modes with effective indices of $n_{eff\,01} = 1.4627176$ and $n_{eff\,11} = 1.4615364$. According to the data collected for the mode conversion switching experiments, the maximum efficiency is obtained at an interference angle corresponding to the grating period and the grating length of about 1.1 mm, which refers to the 434 grating periods. For the given effective indices and the grating period, the Bragg wavelength is calculated 7.41 μm for the reflected mode which is far away from the working wavelength λ (543 nm). The coupling mechanism in this interaction can be explained considering the group I classification in table 1.

Although the frequency matching condition is satisfied, the phase matching requirement is partially satisfied only for one of the Fourier components of the grating having a spatial frequency of $4\pi/L_g$ where L_g is the grating length. For the specified matching condition, the mode conversion efficiency of about %0.34 is measured. Figure 8 illustrates the energy coupling of a mode with effective indices into a mode propagating in the same direction with an effective index $n_{eff\,11}$.

To continue with another source with a wavelength of $\lambda = 632.8$ nm, the fiber supports two modes $n_{eff\,01} = 1.4611506$ and $n_{eff\,11} = 1.4588856$. According to the measured output power variation, the maximum efficiency is obtained at an interference angle of 5.2° which corresponds to the grating period of 1.957 μm,

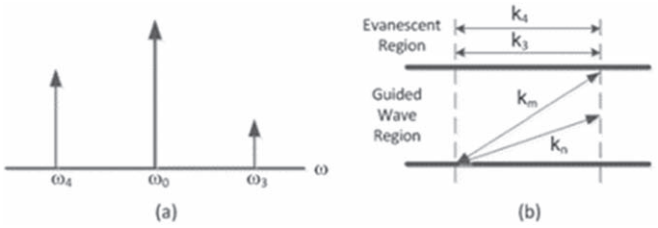

Figure 9. Illustration of a-) frequency matching b-) phase matching.

providing the grating length of about 1 mm. In this case, the mode conversion efficiency of about 0.27% is observed. For the given effective indices and grating period, Bragg wavelength is 5.715 μm for the reflection, which is away from the working wavelength λ. This case suits group I processes, described in table 1. According to the *type I* interaction, the fundamental mode propagating in the optical fiber can be coupled or transferred to the higher-order modes.

4. Discussion on optical switching by wavelength conversion

Power coupling between two light signals having distinctive wavelengths is possible with frequency matching and Quasi-Phase Matching (QPM) [24]. To observe this case, the strong control pulses with wavelength λ_p(532 nm) form the grating on the thin polymer film, and two light signals with wavelengths λ_3(663 nm) and λ_4(440 nm) are launched into the fiber. For each propagating lightwave signal, the fundamental mode excitation in the fiber is ensured. Considering the classical understanding of FWM interactions, the frequency and phase-matching conditions must be satisfied. Two distinct frequencies around the pump frequency having equal propagation vectors in the cladding are shown in figure 9, where ω is the frequency and k is the wave number, respectively.

The frequency matching condition yields the following relation between the wavelengths.

$$\lambda_4 = \frac{1}{\frac{2}{\lambda_p} - \frac{1}{\lambda_3}} \tag{3}$$

Considering the laser bandwidths given in figure 5 and using $\lambda_p = 532$ nm and $\lambda_3 = 663.5$ nm, λ_4 is calculated as $\lambda_4 = 442,\ 06$ nm. All of the values are within the measured limits of the laser bandwidths.

Regarding the geometry in figure 4, the phase-matching condition can be written as

$$\vec{k}_{p1} + \vec{k}_{p2} = \vec{k}_3 + \vec{k}_4 \tag{4}$$

where k_{p1} and k_{p2} are the wave vectors of pump beams, k_3 and k_4 are the wave vectors of the source waves. The components of k_{p1} and k_{p2} in the propagation direction of the source wave cancel each other which implies

$$k_{3z} = -k_{4z} \tag{5}$$

In conventional nonlinear FWM interactions, the wavelength conversion can be achieved by providing the required phase-matching condition in Kerr media via dispersion compensation. However, it was shown that phase-mismatch switching enhances wavelength conversion [22]. In this method, one can vary the medium periodically along the propagation path to obtain quasi-phase-matching (QPM) [22, 23] and provide efficient wavelength conversion. Quantum optical treatment of FWM shows that the phase matching requirement can be expressed in a more general form by an overlap integral of spectral envelopes as in [26].

Here, in this study, the QPM technique by transient modulating the cladding refractive index of the waveguide is considered. Thus, the FWM phase mismatch is compensated by a grating via QPM. Several theoretical investigations have centered on how to realize QPM with such a periodic modulation [25, 27, 28]. In our case, the transient grating can be considered quasi-stationary due to strong pump power and the coupling interaction can be realized given the following condition

$$\beta_4 \pm \beta_3 \pm m\frac{2\pi}{\Lambda} = 0 \tag{6}$$

where Λ is the grating period, $\beta_3 = |k_{3z}|$ and $\beta_4 = |k_{4z}|$ are the propagation constants of the source waves respectively and m is an integer number.

The experiments carried out in this study show that there exists a power transfer from signal λ_3 to signal with wavelength λ_4 and this process occurs only during when the grating period is estimated as $\Lambda = 1.543$ μm. For

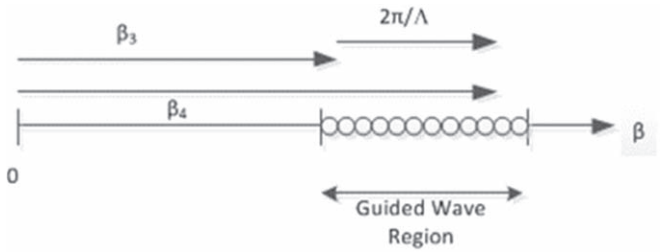

Figure 10. Demonstration of coupling between distinct wavelengths.

$m = 2$ the phase-matching condition given in table 1 for type II interaction is satisfied. This case is illustrated in figure 10.

Considering the experimental results, we may conclude that as a result of the interaction, two photons with frequency ω_0 are annihilated to create two photons with frequencies ω_3 and ω_4, traveling in opposite directions. This causes a decrease in the wave's amplitude with wavelength λ_3 and an increase in the wave's amplitude with wavelength λ_4 as observed in the experimental data.

Although the transient grating has a certain aperiodic interference pattern along the optical fiber, it is moving in the transverse direction, and that pattern casts into a refractive index modulation due to Kerr nonlinearity [29]. The grating points (phase matching) are only moving transversely. In practice due to the finite response of the material (polymer) that grating points get smoother line shapes eventually. Therefore, the transient grating keeps aperiodicity in the longitudinal direction while moving in the transverse direction, having a smooth refractive index profile.

5. Conclusion

A novel all-optical fiber switch has been fabricated and demonstrated. Through interaction in the evanescent nonlinear cladding region, the switching/routing principle of the device based on FWM interactions has been experimentally verified. These results proved the switching capability of the dynamic transient gratings in optical fiber devices.

Considering the device's operation, the optimal design is necessary for minimum power requirement, switching response time, and switching efficiency. Further improvements are expected for experiments with better beam-quality of writing beam. A high-nonlinearity polymeric film (or fiber cladding) can significantly reduce the necessary power of the writing beam. Switching power is in particular crucial for Kerr-type nonlinear devices due to weak optical control signals. Finding the exact minimum power required is difficult since only a fraction of the pump power is effectively involved in the operation. Finally, the complete device operation may need some other components to be integrated such as an address extractor, spectral filter, optical buffer, etc.

This type of device seems especially promising for all-optical network switches, routers, and DWDM applications, where the optical packets need to be switched or routed in fiber among a few output ports. This study has mostly concentrated on proving the principle and it needs optimization for better performance before practical applications.

The dynamic nature of the device operation makes it attractive for many other applications such as a light-by-light switch that may also be regarded as a counterpart of the transistor in electronics.

Data availability statement

All data that support the findings of this study are included within the article (and any supplementary files).

Funding information

This work has been supported in part by the Scientific and Technological Research Council of Turkey (TUBITAK) under research projects 109E240 and 114E006.

ORCID iDs

Osman Akin https://orcid.org/0000-0001-9114-4744

References

[1] Andermahr N and Fallnich C 2010 Optically induced long-period fiber gratings for guided mode conversion in few-mode fibers *Opt. Express* **18** 4411–6
[2] Sahu P 2012 All-optical switch using optically controlled two mode interference coupler *Appl. Opt.* **51** 2601–5
[3] Wang K, Wonfor A, Penty R and White I 2012 Active-passive 4x4 SOA-based switch with integrated power monitoring *Optical Fiber Communication Conf., OSA Technical Digest (Optical Society of America)* paper OTh4F.4
[4] Volz T, Reinhard A, Winger M, Badolato A, Hennessy K J, Hu E L and Imamoğlu A 2012 Ultrafast all-optical switching by single photons *Nat. Photonics* **6** 605–9
[5] Glesk I, Bock P, Cheben P, Schmid J, Lapointe J and Janz S 2011 All-optical switching using nonlinear subwavelength Mach–Zehnder on silicon *Opt. Express* **19** 14031–9
[6] Cook E H *et al* 2020 Polysilicon Grating Switches for LiDAR *J. Microelectromechanical Systems* **29** 1008–13
[7] Hellwig T, Schnack M, Walbaum T, Dobner S and Fallnich C 2014 Experimental realization of femtosecond transverse mode conversion using optically induced transient long-period gratings *Opt. Express* **22** 24951–8
[8] Eggleton B J, Slusher R E, Judkins J B, Stark J B and Vengsarkar A M 1997 All-optical switching in long-period fiber gratings *Opt. Lett.* **22** 883–5
[9] Singh M and Datta A 2018 Modeling of a vertical hybrid plasmonic switch with VO2 fin bragg grating *IEEE Photonics Technol. Lett.* **30** 997–1000
[10] Chen N, Yun B and Cui Y 2006 Cladding index modulated fiber grating *Opt. Commun.* **259** 587–91
[11] Badri S and Farkoush S 2021 Subwavelength grating waveguide filter based on cladding modulation with a phase-change material grating *Appl. Opt.* **60** 2803–10
[12] Shibuya K, Ishii K, Atsumi Y, Yoshida T, Sakakibara Y, Mori M and Sawa A 2020 Switching dynamics of silicon waveguide optical modulator driven by photothermally induced metal-insulator transition of vanadium dioxide cladding layer *Opt. Express* **28** 37188–98
[13] Schneider T and Reif J 2002 Influence of an ultrafast transient refractive-index grating on nonlinear optical phenomena *Phys. Rev. A* **65** 023801
[14] Zhong C, Li J and Lin H 2020 Graphene-based all-optical modulators *Front. Optoelectron* **13** 114–28
[15] Schneider T *et al* 1999 Ultrafast optical switching by instantaneous laser–induced grating formation and self-diffraction in barium fluoride *Applied Physics B, Lasers and Optics* **68** 749–51
[16] Haque S A and Nelson J 2010 Toward organic all-optical switching *Sci.* **327** 1466–7
[17] Zhang X, Hosseini A, Lin X, Subbaraman H and Chen R T 2013 'Polymer-based hybrid-integrated photonic devices for silicon on-chip modulation and board-level optical interconnects *Selected Topics in Quantum Electronics, IEEE Journal of* **19** 196,210
[18] Akin O and Dinleyici M S 2010 An all-optical switching based on resonance breaking with a transient grating *IEEE/OSA J. Lightwave Technology* **28** 3470–7
[19] Akin O and Dinleyici M S 2014 Demonstration of pulse controlled all-optical switch/modulator *Opt. Lett.* **39** 1469–72
[20] He T, Cheng Y, Du Y and Mo Y 2007 Z-scan determination of third-order nonlinear optical nonlinearity of three azobenzenes doped polymer films *Opt. Commun.* **275**
[21] Sabatyan A and Tavassoly M T 2007 Application of Fresnel diffraction to nondestructive measurement of the refractive index of optical fibers *Opt. Eng.* **46** 128001
[22] Boncek R K and Rode D L 1991 Far-field radiation and modal dispersion of 1310 nm dispersion-optimized fiber at 850 nm *J. Lightwave Technol.* **9** 18,21
[23] Erdogan T 1997 Fiber grating spectra *J. Lightwave Technol.* **15** 1277
[24] Lefevre Y, Vermeulen N and Thienpont H 2013 'Quasi-phase-matching of four-wave-mixing-based wavelength conversion by phase-mismatch switching *J. Lightwave Technol.* **31** 2113–21
[25] Driscoll J B, Ophir N, Grote R R, Dadap J I, Panoiu N C, Bergman K and Osgood R M 2012 Width-modulation of Si photonic wires for quasi-phase-matching of four-wave-mixing: experimental and theoretical demonstration *Opt. Express* **20** 9227–42
[26] Ekici C 2021 A study on entangled photon pairs in graded-index optical fibers *Doctoral Dissertation* (Izmir, Turkey: Izmir Institute of Technology) Retrieved from https://hdl.handle.net/11147/11669
[27] Driscoll J B, Grote R R, Liu X, Dadap J I, Panoiu N C and Osgood Jr R M 2011 Directionally anisotropic Si nanowires: on-chip nonlinear grating devices in uniform waveguides *Opt. Lett.* **36** 1416–8
[28] Vermeulen N, Sipe J E, Lefevre Y, Debaes C and Thienpont H 2011 Wavelength conversion based on raman- and non-resonant four-wave mixing in silicon nanowire rings without dispersion engineering *IEEE J. Sel. Top. Quantum Electron.* **17** 1078–91
[29] Eichler H J, Günter P, Pohl and Dieter W 1986 *Laser-Induced Dynamic Gratings* (Berlin: Springer) Chap. 4 subsection 4.7 'Moving Gratings'